Nature of the Volume Isotope Effect in Ice

Koichiro Umemoto, Emiko Sugimura, Stefano de Gironcoli, Yoichi Nakajima, Kei Hirose, Yasuo Ohishi, and Renata M. Wentzcovitch

Phys. Rev. Lett. **115**, 173005 — Published 22 October 2015

DOI: 10.1103/PhysRevLett.115.173005

Nature of the volume isotope effect in ice

Koichiro Umemoto[1,2], Emiko Sugimura[3], Stefano de Gironcoli[4], Yoichi Nakajima[5], Kei Hirose[2,6], Yasuo Ohishi[7], and Renata M. Wentzcovitch[2,4,8]

[1]*Department of Earth Sciences, University of Minnesota, 310 Pillsbury drive SE, Minneapolis, MN 55455, USA*

[2]*Earth-Life Science Institute, Tokyo Institute of Technology, 2-12-1 Ookayama, Meguro-ku, Tokyo, 152-8550, Japan*

[3] *Department of Earth and Planetary Sciences, Tokyo Institute of Technology, 2-12-1 Ookayama, Meguro-ku, Tokyo, 152-8550, Japan*

[4]*Scuola Internazionale Superiore di Studi Avanzati (SISSA) and CNR-IOM DEMOCRITOS Simulation Centre, Via Bononea 265, 34146 Trieste, Italy*

[5]*Materials Dynamics Laboratory, RIKEN SPring-8 Center, RIKEN, 1-1-1 Kouto Hyogo 679-5148, Japan*

[6]*Laboratory of Ocean-Earth Life Evolution Research, Japan Agency for Marine-Earth Science and Technology, Yokosuka, Kanagawa 237-0061, Japan*

[7]*Japan Synchrotron Radiation Research Institute, Sayo-cho, Hyogo 679-5198, Japan*

[8] *Department of Chemical Engineering and Materials Science and Minnesota Supercomputing Institute, University of Minnesota, 421 Washington ave SE, Minneapolis, MN 55455, USA*

(Dated: September 21, 2015)

Abstract

The substitution of hydrogen (H) by deuterium (D) in ice Ih and in its H-ordered version, ice XI, produces an anomalous form of volume isotope effect (VIE), i.e., volume expansion. This VIE contrasts with the normal VIE (volume contraction) predicted in ice-VIII and in its H-disordered form, ice VII. Here we investigate the VIE in ice XI and in ice VIII using first principles quasi-harmonic calculations. We conclude that normal and anomalous VIEs can be produced in ice VIII and ice XI in sequence by application of pressure (ice XI starting at negative pressures) followed by a third type – anomalous VIE with zero point (ZP) volume contraction. The latter should also contribute to the isotope effect in the ice VII $\rightarrow$ ice X transition. The predicted change between normal an anomalous VIE in ice VIII at 14.3 GPa and 300 K is well reproduced experimentally using x-ray diffraction measurements. The present discussion of the VIE is general and conclusions should be applicable to other solid phases of H_2O, possibly to liquid water under pressure, and to other H-bonded materials.

PACS numbers:

Ice Ih, the common form of ice at ambient pressure, has two well-known intriguing properties originating in its vibrational spectrum: a) the well-known negative thermal expansion (NTE) coefficient and b) an anomalous volume isotope effect (VIE). Normally, volume expands with increasing temperature. But, the volume of ice Ih contracts below $\sim$ 70 K [1]. NTE is also observed in other materials: silicon, germanium, silica, and graphite (graphene), to mention a few.

The origin of NTE has been addressed quite successfully theoretically using the quasi-harmonic approximation (QHA) [2–6]. The QHA is based on a phonon gas model, where phonon frequencies depend on volume but not on temperature. The QHA Helmholtz free energy is then [7]:

$$F(V,T) = E_0(V) + \frac{1}{2}\sum_{i,\mathbf{q}} \hbar\omega_{i,\mathbf{q}}(V) + \sum_{i,\mathbf{q}} k_B T \log\left[1 - \exp\left(-\frac{\hbar\omega_{i,\mathbf{q}}(V)}{k_B T}\right)\right]. \qquad (1)$$

$E_0(V)$ is the total energy of static nuclei in relaxed atomic configurations at volume V and $\omega_{i,\mathbf{q}}$ are phonon frequencies of the i-th mode at wave vector $\mathbf{q}$. Second and third terms in the r.h.s. of Eq. 1 are contributions from the zero-point motion (F_{ZP}) and thermal excitations (F_{th}), respectively. The equilibrium volume, $V_0(T)$, is obtained when $\left.\frac{\partial F}{\partial V}\right|_T = 0$. The volume dependence of phonon frequencies, or Grüneisen parameters, $\gamma_i = -\frac{V}{\omega_i}\frac{\partial \omega_i}{\partial V}$, play a central role in the NTE and in the VIE. In the QHA, thermal expansivity, $\alpha = \frac{1}{V}\left.\frac{\partial V}{\partial T}\right|_P$, can be approximately decomposed into contributions from individual phonons [8]. NTE occurs when the contribution of low-frequencies modes with negative γ_is dominates over those of other modes in the thermal pressure (P_{th}), i.e., the negative volume derivative of F_{th}. Ice Ih has low frequency translational modes ($<\sim$50 cm^{-1}) with negative γ_is that produce the NTE below $\sim$ 70 K [3, 6, 9].

The second intriguing property, the VIE, is the subject of the present Letter. Normally, the volume contracts by substitution of lighter by heavier isotopes. However, the volume of ice Ih expands by replacing hydrogen (H) by deuterium (D) [1]. Recently, the VIEs in ice Ih/XI [6, 10] and in ice VIII [10] were addressed by first principles calculations (brief overview of ice phases is given in Ref. [11]). Pamuk *et al.* [6] convincingly showed that the VIE in ice Ih/XI is caused by high-frequency intra-molecular O-H stretching modes with negative γ_is. These negative γ_is are peculiar to hydrogen-bonded (H-bonded) systems and arise from the anti-correlation between the H-bond (H$\cdots$O) and intra-molecular H-O bond

lengths [11–15]. Volume compression decreases the H$\cdots$O bond-length, weakens H-O bonds increasing their bond-lengths, and decreases H-O stretching mode frequencies [11, 16–19]. Given this common behavior in different forms of H-bonded ice, one might expect the VIE to be anomalous in all ice phases. But, in ice VIII and VII (the H-disordered form of ice VIII), it was computationally demonstrated that the VIE at 0 GPa is normal ($V(H_2O) > V(D_2O)$) [10, 20]. The different nature of the VIE in ice Ih/XI and VII/VIII suggests the relationship between the VIE and stretching modes with negative γ_is is not so simple.

Here we describe the origin of this difference in the VIEs of ice XI and ice VIII by means of first principles QHA calculations at high pressures. We conclude that the presence of stretching modes with negative γ_is is necessary but not sufficient to produce the anomalous VIE. Interestingly, we find three types of VIEs in ice VIII in different pressure ranges: normal, anomalous, anomalous with zero-point (ZP) volume contraction. The VIE in ice VII is also investigated experimentally using x-ray diffraction measurements under pressure and supports the theoretical picture.

Our first principles calculations used norm-conserving pseudopotentials [21] and the Perdew-Burke-Ernzerhof (PBE) form of generalized-gradient approximation for exchange and correlation (XC) [22]. The choice of XC functional is important for the description of H-bonded molecular crystals [11]. Other XC functionals were tested in previous studies [6, 10], including some with van der Waals interaction explicitly accounted for [23–26], but they do not necessarily improve the equation of state of ice VIII and do not change the nature of the VIEs described as a percentagewise change. Therefore, the PBE functional is adequate for the present purpose. A plane-wave basis set with a cutoff energy of 100 Ry was used. The number of **k** points in the irreducible wedge of the Brillouin zones of ice XI and VIII were 6 and 11, respectively. Lattice constants and atomic coordinates were fully optimized at all pressures [27, 28]. Dynamical matrices were computed at $2\times2\times2$ **q**-meshes using density-functional perturbation theory [29, 30]. Phonon frequencies were obtained by interpolation on $12\times12\times8$ and $12\times12\times12$ **q**-point meshes for ice XI and VIII, respectively. All calculations were performed using the Quantum-ESPRESSO software [31].

It is useful first to review the relationship between the structures of ice XI and ice VIII [32]. They are low temperature H-ordered versions of H-disordered ice Ih and ice VII. Ice Ih has hexagonal symmetry. The oxygen sub-lattice has the same atomic arrangement of the fourfold coordinated wurtzite structure. This atomic arrangement is typical of low-

density ice. In the H-ordered version, ice XI, the lattice distorts and acquires orthorhombic symmetry [33, 34]. Oxygen forms two strong intra-molecular H-O bonds with two closer hydrogens and two weak H$\cdots$O bonds with two more distant hydrogens strongly bonded to neighboring oxygens. This rule applies whether hydrogens are ordered or disordered [35]. The structures of ice VII and VIII consist of two inter-penetrating diamond-like oxygen sub-lattices with H-disordered and H-ordered sub-lattices, respectively [36]. This structure is referred to as a self-clathrate. Ice VII has cubic symmetry and VIII is tetragonal. The calculated zero pressure H$\cdots$O bond-lengths in ice XI and VIII are 1.68 Å[37] and 1.98 Å[15]. Longer H$\cdots$O bonds produce shorter and stronger H-O bonds, higher stretching mode frequencies, and less negative stretching-mode γ_is [11, 16–19].

The key role H$\cdots$O bond-lengths play in the nature of the VIE can be investigated using pressure. Fig. 1(a) shows that at 0 GPa $V(D_2O) > V(H_2O)$ in ice XI, i.e., the VIE is anomalous, consistent with previous experimental and theoretical reports [1, 6, 10]. Under pressure, H$\cdots$O bonds contract, H-O bond expands, stretching mode frequencies decrease [11, 16–19], and the anomalous VIE is enhanced. For $P \gtrsim 3$ GPa or $P < -1$ GPa, there are structural instabilities and the VIE cannot be investigated. For $-1 < P < 0$ GPa the VIE remains anomalous but tends towards normal with decreasing pressure. Temperature plays a negligible role in the VIE, indicating that the origin of the VIE can be investigated by analyzing ZP pressure (P_{ZP}) alone [10].

The behavior of the VIE in ice VIII is more complex than in ice XI, as shown in Fig. 2(a). For $P \lesssim 20$ GPa the VIE is normal, consistent with previous results in ice VIII [10, 20] and ice VII [20]. However, For $P \gtrsim 20$ GPa the VIE is anomalous. This *change* in the nature of VIE contrasts with expectations based on results obtained at 0 GPa [10]. To the best of our knowledge, this pressure-induced change in the nature of VIE in ice VIII has not been previously reported.

To address this intricate nature of the VIE in ice XI/Ih and VIII/VII, it is appropriate to invoke P_{ZP}, the negative volume derivative of the second term in Eq. 1:

$$P_{ZP} = -\sum_{i,\mathbf{q}} \frac{\hbar}{2} \frac{\partial \omega_{i,\mathbf{q}}}{\partial V} = \sum_{i,\mathbf{q}} \frac{\hbar}{2} \frac{\omega_{i,\mathbf{q}} \gamma_{i,\mathbf{q}}}{V}. \tag{2}$$

P_{ZP} is considerably larger than P_{th} and essentially defines the nature of the VIE. P_{th} is responsible for the NTE [2–4], but plays a negligible role in the VIE (see Fig. 1a and 2a). Negative P_{th} and NTE are caused by the predominance of low frequency translational modes

with negative γ_i^T, but they play minimal role in the VIE.

It is therefore useful to focus on P_{ZP} and decompose it into contributions from four phonon groups: translational (T), librational (L), bending (B), and stretching (S) modes, as shown in Figs. 1(b) and 2(b) for ice XI and VIII, respectively (see Ref. [11] for vibrational density of states). In both ice XI and VIII, T- and L-modes contribute to increase P_{ZP} while B-modes contribute negligibly. S-modes with negative γ_is decrease P_{ZP}. In ice XI, $P_{ZP}^{H_2O} < P_{ZP}^{D_2O}$ for $P > 0$ GPa, which causes the anomalous VIE. This effect can be clearly attributed to the predominance of S-modes. However, there is one unexpected feature: $P_{ZP}^{H_2O}$ and $P_{ZP}^{D_2O}$ are both negative at 2 GPa, indicating that *ZP motion can cause volume contraction* at high pressures. This effect cannot be experimentally detected but its existence should be acknowledged and its origin understood since experiments provide guidance for improvements of theoretical descriptions of condensed phases of water. It is usually assumed that ZP motion causes volume expansion and predictions by static calculations should underestimate volume somewhat. This is not necessarily the case in ice and possibly in liquid water under pressure.

Ice VIII displays three types of VIE, as indicated in Fig. 2. For $P \lesssim 20$ GPa, despite the existence of S-modes with negative γ_is, T- and L-modes with positive γ_i predominate and $P_{ZP}^{H_2O} > P_{ZP}^{D_2O} > 0$. This results in ZP volume expansion and normal VIE (Fig. 3(a)). At ∼20 GPa, $P_{ZP}^{H_2O} = P_{ZP}^{D_2O} > 0$ and no VIE occurs. For $P \gtrsim 50$ GPa, S-modes with negative γ_is predominate and $P_{ZP}^{H_2O} < P_{ZP}^{D_2O} < 0$, leading to anomalous VIE and ZP volume contraction (Fig. 3(c)). For $20 \lesssim P \lesssim 50$ GPa, there is a continuous change between these VIE types.

These calculations reveal a systematic trend in the VIE of ice phases that correlates with H$\cdots$O bond lengths in each structure (see Fig. 3). The expected sequence of pressure induced VIE types should be: normal VIE with ZP volume expansion → anomalous VIE with ZP volume expansion → anomalous VIE with ZP volume contraction. The first kind does not materialize in ice XI at 0 GPa since its H$\cdots$O bond length is already sufficiently short and S-mode γ_is sufficiently negative to produce anomalous VIE. However, our results indicate that this sequence of VIE types still holds for ice XI, with VIE tending to normal at negative pressures with larger volume. Ice VIII, though denser, has longer H-bond lengths and more negative S-mode γ_is. Densification with simultaneous increase of bond lengths is the natural type of structural change induced by pressure or cooling. In non-molecular

materials, this is accomplished by producing more closed-packed structures with increased atomic coordination.

The nature of the VIE is basically independent of hydrogen ordering. Specifically, the anomalous VIE was shown in both ice Ih and XI at 0 GPa [6, 10]. Similarly, the pattern of VIEs calculated here in ice VIII is analogous to that predicted in ice VII [11, 20]. Therefore, this sequence of VIE types can be investigated experimentally either in ice VII or VIII. Ice VII is more convenient for experimental investigations because it is stable at 300 K. As such, we measured the volumes of both H_2O- and D_2O-ice VII at room temperature under pressure using x-ray diffraction (XRD). Ice VII/VIII is a good experimental target for this investigation because it has a pressure stability field much wider than ice Ih/XI.

Very similar experimental techniques were used for measurements of H_2O- and D_2O-ice. High pressure conditions were achieved in a diamond anvil cell with flat 300-μm culet diamond anvils. Liquid H_2O and D_2O with 99.9+% purity were purchased from Seiki Co., Ltd and Wako Pure Chemical Industries, Ltd, respectively. Either H_2O or D_2O into a hole drilled in a pre-indented rhenium gasket with a toroidal-shaped thin gold (Au) foil with 3 to 5-μm thickness. The Au foil served as both a laser absorber for thermal annealing and as internal pressure standard for both H_2O and D_2O [38]. The volume data were collected for H_2O- and D_2O-ice VII upon increasing pressure. After each pressure increment except at 8 GPa for H_2O in Run 1, both H_2O and D_2O sample was laser annealed by heating the Au foil up to 1300 K, typically for 3 minutes. Angle-dispersive XRD spectra were then collected at 300 K using an x-ray energy of 30 keV at the beamline BL10XU of SPring-8. The x-ray wavelength and camera distance were calibrated by using an identical CeO_2 standard for both H_2O and D_2O measurements. Two separate sets of compression experiments were conducted each for H_2O (4 to 39 GPa) and D_2O (3 to 35 GPa), respectively (STable II). The volumes of ice VII were obtained from 110, 200, and 211 peaks of the body-centered-cubic structure for both H_2O and D_2O, except for the 211 line at 39 GPa in H_2O because of peak overlap. Pressures were determined from the unit-cell parameter of Au calculated from 111, 200, 220, 311, and 222, except for the data taken at 35-39 GPa in which 220 and 311 peaks were unavailable owing to the limited two-theta angle. Previously a possibility of symmetry lowering of ice VII beyond 14 GPa was reported [39]. To check how it could affect volume, we performed a full-profile Rietveld fitting for an XRD data at 17.4 GPa. But it did not give volume difference larger than error.

The experimental compression curves of H_2O- and D_2O-ice VII are plotted in Fig. 4(a). Figure 4(b) shows that the VIE changes from normal to anomalous at ∼16 GPa, confirming the theoretical prediction. The calculated pressure for this change in ice VIII is ∼14.3 GPa at 300 K (∼20 GPa at 0 K), in outstanding agreement with measurements. This discussion of the VIE based on P_{ZP} should be applicable to other H-bonded phases, including liquid water under pressure. Broadly speaking, materials containing X-H$\cdots$X type of bonds should display more normal (anomalous) VIE for smaller (larger) X-H to H$\cdots$X bond-lengths ratios. Finally, the VIE in ice VIII/VII should also be related to another observed kind of hydrogen isotope effect - that on the transition pressure between ice VIII/VII and ice X [16, 18]. This transition involves H-bond symmetrization [12] and tunneling of hydrogen [13, 40, 41] through the barrier separating the two minima of the double potential well between two oxygens. The transition pressure in D_2O-ice, ∼75 GPa, is higher than that in H_2O-ice VIII, ∼65 GPa, [16, 18]. At same bond lengths, tunneling by H is more likely than by D and this should contribute to some extent to the isotope effect on the transition pressure. However, the smaller volume contraction in D_2O-ice VIII (or VII) caused by its less negative P_{ZP} (see Fig. 3c) should also increase the transition pressure by replacing H by D in ice VIII.

Acknowledgments

KU and RMW were supported also by NSF under EAR-0757903 and EAR-1019853. Calculations were performed at the Minnesota Supercomputing Institute, at the Laboratory for Computational Science and Engineering at the University of Minnesota, and at the Blue Water system at NCSA. XRD experiments were performed at SPring-8 (proposal no. 2013A0087 and 2014B0080).

[1] K. Röttger, A. Endriss, J. Ihringer, S. Doyle, and W. F. Kuhs, Acta Cryst. B**50**, 644 (1994).

[2] C. H. Xu, C. Z. Wang, C. T. Chan, and K. M. Ho, Phys. Rev. B **43**, 5024 (1991).

[3] H. Tanaka, J. Chem. Phys. **108**, 4887 (1998).

[4] J. Xie, S. P. Chen, J. S. Tse, S. de Gironcoli, and S. Baroni, Phys. Rev. B **60**, 9444 (1999).

[5] N. Mounet and N. Marzari, Phys. Rev. B **71**, 205214 (2005).

[6] B. Pamuk, J. M. Soler, R. Ramirez, C. P. Herrero, P. W. Stephens, P. B. Allen, and M. V. Fernandez-Serra, Phys. Rev. Lett. **108**, 193003 (2012).

[7] D. Wallace, *Thermodynamics of Crystals*, John Wiley, Hoboken, N. J. (1972).

[8] B. B. Karki and R. M. Wentzcovitch, Phys. Rev. B **68**, 224304 (2003).

[9] Th. Strässle, A. M. Saitta, S. Klotz, and M. Braden, Phys. Rev. Lett. **93**, 225901 (2004).

[10] È. D. Murray and G. Galli, Phys. Rev. Lett. **108**, 105502 (2012).

[11] See Supplemental Material [url], which includes Refs. [42-53].

[12] W. B. Holzapfel, J. chem. Phys. **56** 712 (1972).

[13] M. Benoit, D. Marx, and M. Parrinello, Nature **392**, 258 (1998).

[14] J. M. Besson, Ph. Pruzan, S. Klotz, G. Hamel, B. Silvi, et al., Phys. Rev. B 49, 12540 (1994)

[15] K. Umemoto and R. M. Wentzcovitch, Phys. Rev. B 69, R180103 (2004).

[16] Ph. Pruzan, E. Wolanin, M. Gauthier, J. C. Chervin, B. Canny, D. Häuesermann, and M. Hanfland, J Phys Chem B **101**, 6230 (1997).

[17] A. F. Goncharov, V. V. Struzhkin, H. K. Mao, and R. J. Hemley, Phys. Rev. Lett. 83, 1998 (1999).

[18] M. Song, H. Yamawaki, H. Fujihisa, M. Sakashita, and K. Aoki, Phys Rev B **68**, 014106 (2003).

[19] K. Umemoto and R. M. Wentzcovitch, Phys. Rev. B 71, 012102 (2005).

[20] K. Umemoto, R. M. Wentzcovitch, S. de Gironcoli, and S. Baroni, Chem. Phys. Lett. **499**, 236 (2010).

[21] N. Troullier and J. L. Martins, Phys. Rev. B **43**, 1993 (1991).

[22] J. P. Perdew, K. Burke, and M. Ernzerhof, Phys. Rev. Lett. **77**, 3865 (1996).

[23] Y. Zhang and W. Yang, Phys. Rev. Lett. **80**, 890 (1998).

[24] M. Dion, H. Rydberg, E. Schroder, D. C. Langreth, and B. I. Lundqvist, Phys. Rev. Lett. **92**,

246401 (2004).

[25] K. Lee, E. D. Murray, L. Kong, B. I. Lundqvist, and D. C. Langreth, Phys. Rev. B **82**, 081101 (2010).

[26] J. Wang, G. Roman-Perez, J. M. Soler, E. Artacho, and M.-V. Fernandez-Serra, J. Chem. Phys. **134**, 024516 (2011).

[27] R. M. Wentzcovitch, Phys. Rev. B **44**, 2358 (1991).

[28] R. M. Wentzcovitch, J. L. Martins, and G. D. Price, Phys. Rev. Lett. **70**, 3947 (1993).

[29] P. Giannozzi, S. de Gironcoli, P. Pavone, and S. Baroni, Phys. Rev. B **43**, 7231 (1991).

[30] S. Baroni, S. de Gironcoli, A. Dal Corso, and P. Giannozzi, Rev. Mod. Phys. **73**, 515 (2001).

[31] P. Giannozzi, et al., J. Phys. Condens. Matter **21**, 395502 (2009).

[32] K. Umemoto and R. M. Wentzcovitch, Chem. Phys. Lett. **405**, 53 (2005).

[33] A. J. Leadbetter, R. C. Ward, J. W. Clark, P. A. Tucker, T. Matsuo, and H. Suga, J. Chem. Phys. 82, 424 (1985).

[34] R. Howe and R. W. Whitworth, J. Chem. Phys. 90, 4450 (1989).

[35] L. Pauling, J. Am. Chem. Soc. **57**, 2680 (1935).

[36] W. F. Kuhs, J. L. Finney, C. Vettier, and D. V. Bliss, J. Chem. Phys. 81, 3612 (1984).

[37] K. Umemoto, R. M. Wentzcovitch, S. Baroni, and S. de Gironcoli, Phys. Rev. Lett. 92, 105502 (2004).

[38] Y. Fei, A. Ricolleau, M. Frank, K. Mibe, G. Shen, and V. Prakapenka, Proc. Nat. Acad. Sci. **104** 9182 (2007).

[39] M. Somayazulu, J. Shu, C. Zha, A. F. Goncharov, O. Tschauner, H. K. Mao, and R. J. Hemley, J. Chem. Phys. **128**, 064510 (2008).

[40] J. A. Morrone, L. Lin, and R. Car, J. Chem. Phys. **130**, 204511 (2009).

[41] Y. Bronstein, P. Depondt, F. Finocchi, and A. M. Saitta, Phys. Rev. B **89**, 214101 (2014).

[42] V. F. Petronko and R. W. Whitworth, *Physics of ice* (Oxford Univ. Press, Oxford, 1999) and references therin.

[43] Y. Tajima, T. Matsuo, and H. Suga, Nature **299**, 810 (1982).

[44] C. Lobban, J. L. Finney, and W. F. Kuhs, Nature **391**, 268 (1998).

[45] C. G. Salzmann, P. G. Radaelli, A. Hallbrucker, E. Mayer, and J. L. Finney, Nature **311**, 1758 (2006).

[46] C. G. Salzmann, P. G. Radaelli, E. Mayer, and J. L. Finney, Phys. Rev. Lett. **103**, 105701

(2009).

[47] A. Falenty, T. C. Hansen, and W. F. Kuhs, Nature **516**, 231 (2014).

[48] K. Umemoto, Rev. Mineral. Geochem. **71**, 315 (2010).

[49] D. R. Hamann, Phys. Rev. B **55**, R10157 (1997).

[50] J. P. Perdew and Y. Wang, Phys. Rev. B **45**, 13115 (1992).

[51] E. Sugimura, T. Iitaka, K. Hirose, K. Kawamura, N. Sata, and Y. Ohishi, Phys. Rev. B **77**, 214103 (2008).

[52] C. S. Zha, H. K. Mao, R. J. Hemley, and T. S. Duffy, Rev. High Pressure Sci. Technol., Vol. 7, pp. 739-741 (1998).

[53] M. Song, A. Yoneda, and E. Ito, Chinese Sci. Bull. **52**, 1600 (2007).

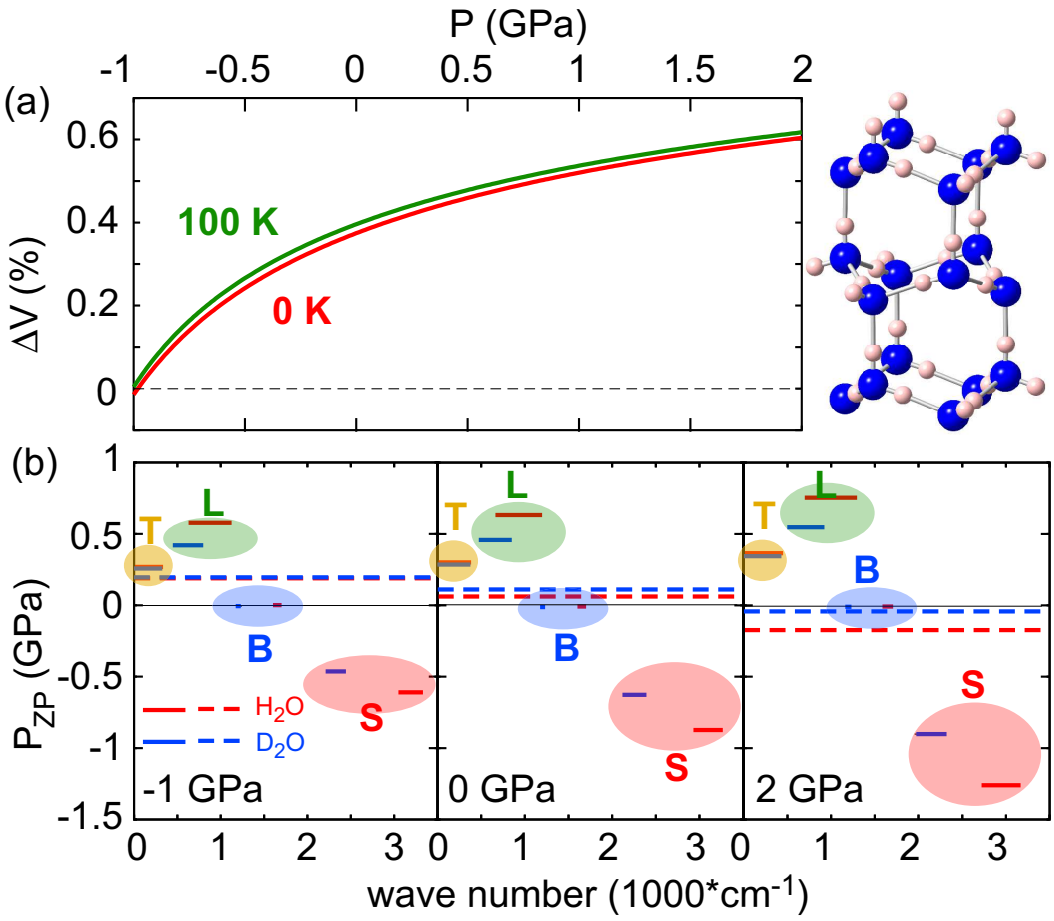

FIG. 1: (a) Calculated percentage volume difference between D_2O- and H_2O-ice XI: $\Delta V(\%) = \left[\frac{V(D_2O) - V(H_2O)}{V(H_2O)}\right] * 100$. (b) Total zero-point pressure, P_{ZP} (dashed lines), and contributions from distinct types of mode ("T": Translational, "L": Librational, "B": Bending, and "S": Stretching mode) at -1 GPa, 0 Gpa, and 2 GPa. Blue and red dashed lines represent zero-point pressures for H_2O and D_2O, respectively.

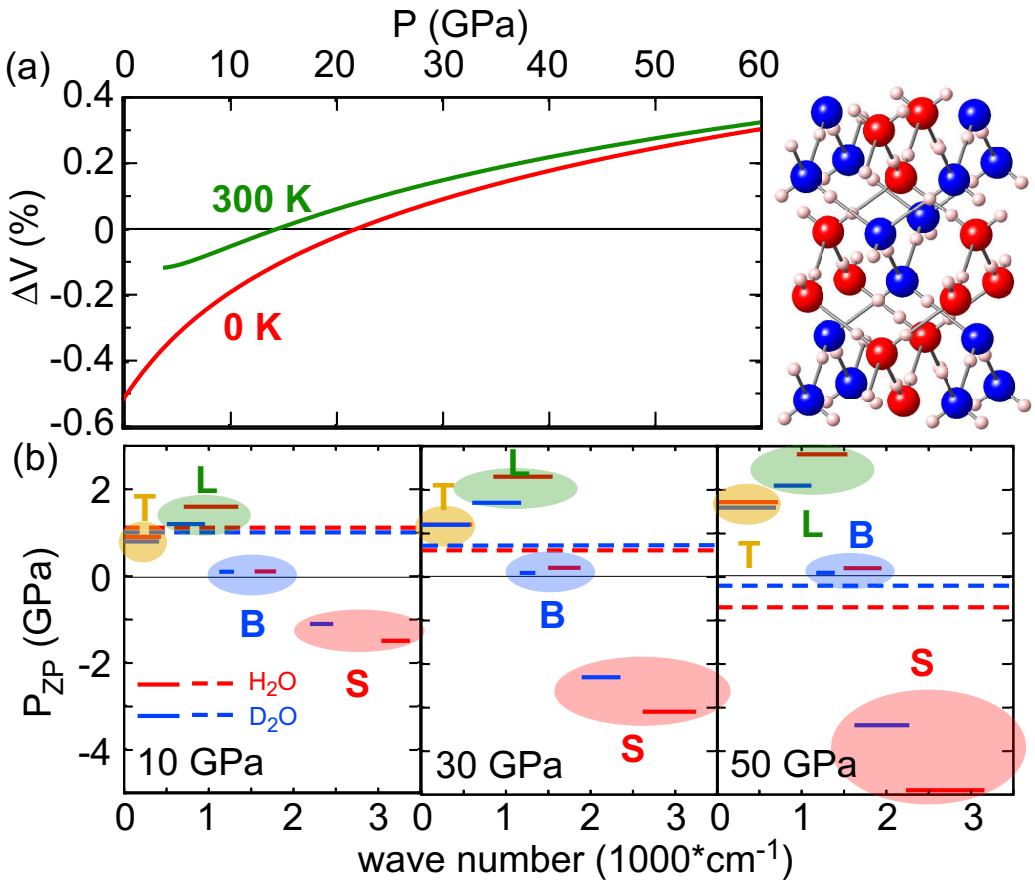

FIG. 2: Same as Fig. 1 but for ice VIII. See Fig. 1 caption for details.

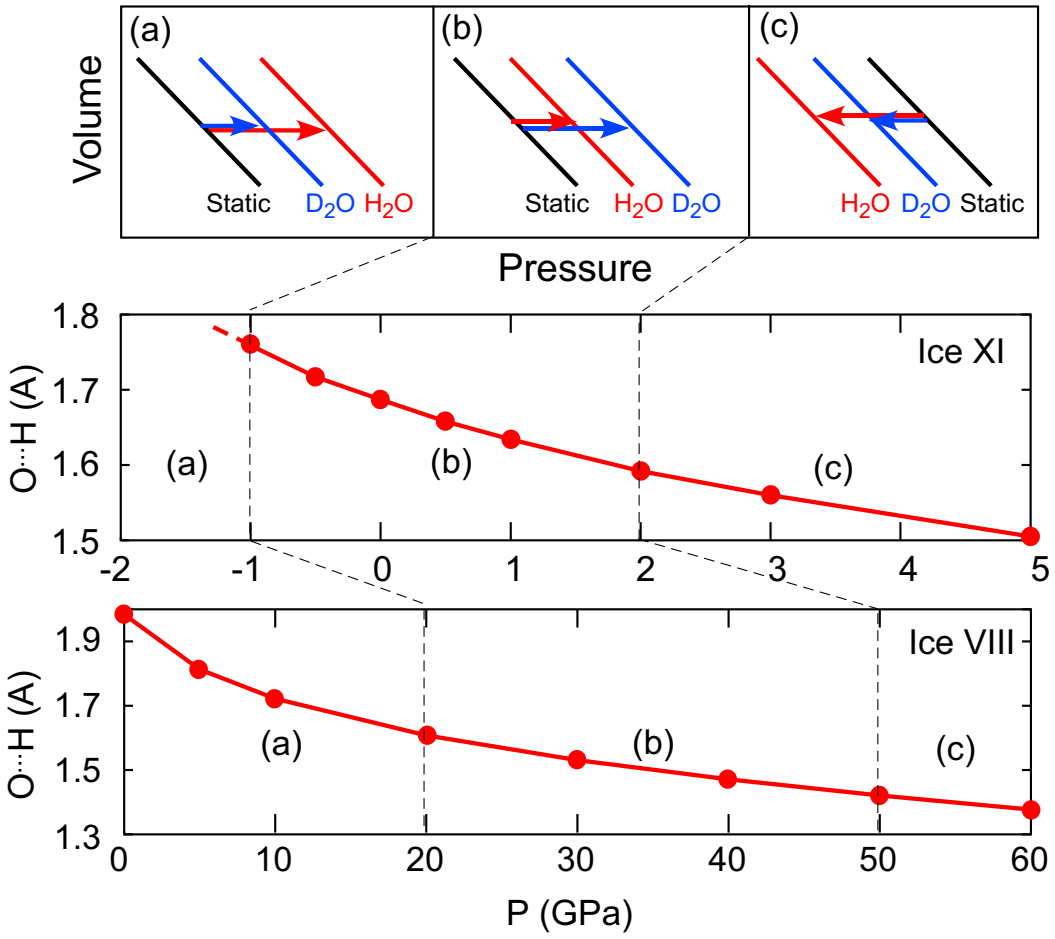

FIG. 3: Schematic representation of the VIE and calculated H-O bond lengths in ice XI and VIII. The types of VIE are (a) normal, (b) anomalous with ZP volume expansion, and (c) anomalous with ZP volume contraction.

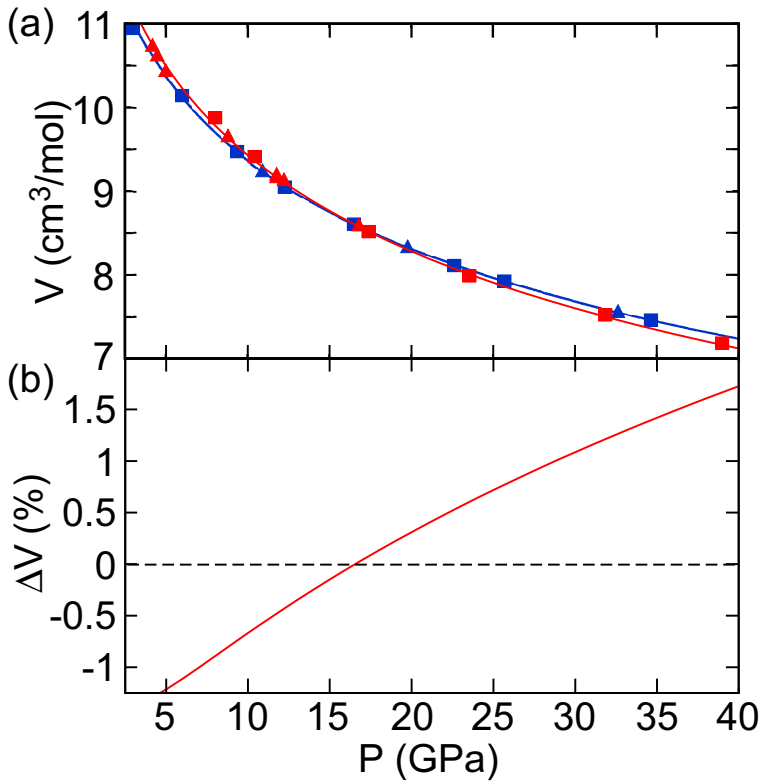

FIG. 4: (a) Molar volumes of H_2O- (red) and D_2O-ice VII (blue) obtained in XRD measurements. Squares and triangles denote results of different compression runs. Experimental errors in both pressure and volume are smaller than or comparable to symbol sizes. The red and blue solid lines are Vinet EOS fitted to the data; $P = 3K_0x^{-2}(1-x)\exp\left[\frac{3}{2}(K'-1)(1-x)\right]$, where $x = (V/V_0)^{1/3}$ and V_0, K_0, and K' are molar volume, isothermal bulk modulus, and its pressure derivative, respectively, at 0 GPa and room temperature. Least square fittings yielded $V_0 = 13.27$ cm^3/mol, $K_0 = 10.36 \pm 1.8$ GPa, and $K' = 6.38 \pm 0.33$ for H_2O and $V_0 = 13.25 \pm 0.3$ cm^3/mol, $K_0 = 8.52 \pm 1.53$ GPa, and $K' = 7.39 \pm 0.29$ for D_2O. (b) Percentage volume difference, $\Delta V(\%) = \left[\frac{V(D_2O) - V(H_2O)}{V(H_2O)}\right] * 100$, inferred from these EOSs.